Investigation of the Effect of Deep Cryogenic Process on the Tribological Properties of X153CrMoV12 Mold Steel

Sıtkı Akıncıoğlu (iD)

This study investigated the effect of deep cryogenic treatment (-140 °C) on the wear resistance, hardness, wear rate and electrical conductivity of X153CrMoV12 steel. The results showed that with deep cryogenic treatment, the friction coefficient was increased by 64.67% compared to that of traditional heat treatment. In addition, it was observed that fine carbide was formed, the carbide rate increased, and the particles were homogeneously dispersed by the deep cryogenic treatment. The difference in the wear rate of deep cryogenic treatment 2 (Cry-2) and deep cryogenic treatment 1 (Cry-1) sample was 33.6 and 29.6% higher than that of the conventional heat treatment (CHT) sample, respectively. The microhardness value of Cry-2 and Cry-1 sample was 9.9 and 8.3% higher than that of the CHT sample, respectively. With Cry-2, the wear rate was reduced by 50.7% compared to CHT samples.

1. Introduction

Deep cryogenic treatment is a heat treatment applied at -140 and -196 °C. As a method that improves the mechanical and tribological properties (hardness, toughness, wear resistance, microstructure, etc.) of materials, its application field has expanded in recent years (Ref 1). It is used in the development of mechanical and tribological properties in ferrous and nonferrous metal alloys, ceramics, plastics, cold work and hot work tool steels, composite material, copper, high speed steels and cutting tools (Ref 2-8). Properties such as hardness, toughness, wear resistance and wear rate are improved as a result of cryogenic treatment (Ref 9-12). In order to obtain the maximum effect from cryogenic treatment, application parameters differ depending on the properties of the material to be treated. Parameters such as cryogenic soaking temperature, soaking time and tempering processes should be determined appropriately. Otherwise, the expected improvements in mechanical and tribological properties of the materials may not be achieved (Ref 1).

In recent years, cryogenic treatments have been applied to materials using many different parameters (Ref 13-15). For example, Das et al. (Ref 2) investigated its effect on carbide formation and tribological properties by applying deep cryogenic treatment to AISI D2 steel. They applied traditional quenching and tempering to one sample and deep cryogenic treatment to the other and compared these two processes. They performed the deep cryogenic treatment for 36 and 84 h at -196 °C, followed by 2 h of tempering at 200 °C. They applied traditional quenching and tempering to one sample and deep

cryogenic treatment to the other and compared these two processes. They concluded that the deep cryogenic treatment caused a remarkable change in the microstructure in addition to a change in the tribological properties. Çiçek et al. (Ref 16) investigated the effects of deep cryogenic processing on the wear behavior and mechanical properties (hardness and wear resistance) of AISI H13 tool steel. They compared the effects of traditional heat treatment, deep cryogenic process and cryogenic treatment + tempering process. They applied the deep cryogenic treatment at -145 °C for 24 h. The abrasion tests were carried out in dry conditions using two loads of 60 and 80 N, two sliding speeds of 0.8 and 1 m/s, and a wear distance of 1000 m on a pin-on-disk test device. Thanks to the deep cryogenic process, 12% increase in wear resistance and 24% increase with deep cryogenic process + tempering were achieved. They determined that these results were caused by the formation of small size and homogeneously dispersed carbide particles and the transformation of the retained austenite into martensite. Amini et al. (Ref 17) applied shallow (-80 °C) and deep (-196 °C) cryogenic treatment to 80CrMo125 tool steel. The results showed that the deep cryogenic treatment reduced the residual austenite. They found that the waiting time of 36 h contributed more to the wear resistance and that the deep cryogenic treatment significantly increased the wear resistance and the carbide ratio, thus ensuring homogeneous dispersion. Das et al. (Ref 18) compared the effect of cold treatment (-80 °C), deep cryogenic treatment (-196 °C) and conventional heat treatment on the wear resistance of AISI D2 steel. Hardening and tempering were applied at 1025 and 200 °C, respectively. The results indicated a remarkable increase in the wear resistance with the deep cryogenic treatment compared to the cold treatment and conventional heat treatment. Amine et al. (Ref 19) investigated the effect of deep cryogenic treatment (-196 °C for 48 h.) on the hardness, microstructure and wear resistance of AISI D2 steel. After the cryogenic treatment, the samples were tempered at 180 °C for 3 h. The values obtained were considered as a reference for conventional heat-treated samples. The deep cryogenic treatment eliminated retained austenite, increased the amount of carbide and provided better carbide distribution. Korade et al. (Ref 20) investigated the effect of deep cryogenic

Sıtkı Akıncıoğlu, Department of Machine Design and Construction, University of Düzce, 81700 Düzce, Turkey. Contact e-mails: sitkiakincioglu@duzce.edu.tr and sitkiakincioglu@gmail.com.

treatment (−185 °C for 36 h.) applied before and after tempering (210 °C for 2 h.) on the friction and wear behavior of AISI D2 steel. They tried different combinations of heat and cryogenic treatments and achieved optimum friction and wear results with cryogenic treatment and a single tempering process. Oppenkowski et al. (Ref 21) applied a deep cryogenic treatment (−196 °C for 36 h.) to AISI D2 steel in addition to conventional heat treatment. They achieved the lowest wear rate with the 36-h cryogenic cool-down. Güneş et al. (Ref 22) investigated the effect of deep cryogenic treatment (−145 °C) on the wear resistance of AISI 5200 bearing steel. They investigated the effect of cryogenic treatment holding times (12, 24, 36, 48, 60 hours). They performed the experiments in a ball-on-disk tester under 10 N and 20 N loads at 0.15 m/s sliding velocity. They determined the most effective holding time in wear resistance of 36 hours. During this holding time, they reached the highest hardness value, the lowest wear rate and coefficient of friction. Das et al. (Ref 23) investigated the effect of deep cryogenic treatment soaking time (−196 °C for 0-132 h) on the wear properties, hardness and microstructure of AISI D2 steel. According to the microstructure and wear results, the ideal soaking time was 36 h. Studies on the commonly used AISI D2, in general, involve comparisons of shallow to deep cryogenic treatment and optimization of cryogenic treatment soaking time (Ref 24, 25). Different effects on mechanical and microstructural properties were obtained with each parameter change. In these studies, it was observed that the cryogenic process application parameters could not be determined for the best performance. In other words, for cryogenic treatment, the application method and duration which yield the best performance (wear resistance, hardness, toughness, etc.) remain undetermined. Therefore, studies on the optimization of cryogenic process parameters to increase the mechanical and tribological properties of X153CrMoV12 steel of deep cryogenic process are continuing.

In this study, different cryogenic treatments were applied to X153CrMoV12 cold work mold steel, and the effects on the hardness, wear rate, coefficient of friction, microstructure and electrical conductivity were investigated. Unlike the studies in the literature, tempering was applied at 150, 500 and 520 °C. In addition, deep cryogenic treatment was applied at a different temperature (− 140 °C) and performed before and after the first tempering, and thus, the effect of the order of application was also investigated.

2. Material and Methods

Samples of X153CrMoV12 cold work tool steel (Ø15mm × 20 mm bar) were used in this study. The samples of X153CrMoV12 steel contain 1.4% C, 0.3% Mn, 0.03% P, 0.03% S, 0.04% Si 12% Cr, 0.7% V, 0.8% Mo and Fe in balance. Samples are coded as; untreated sample (UT), conventional heat treatment sample (CHT), deep cryogenic treatment sample 1 (Cry-1) deep cryogenic treatment sample 2 (Cry-2). Samples were subjected to conventional heat treatment and deep cryogenic treatment in two different sequences. Heat treatments applied to the samples are given in Table 1. Deep cryogenic treatment (−140 °C/120 min) was carried out in a nitrogen atmosphere. The effect of deep cryogenic treatment and the cryogenic treatment sequence on the tribological properties of the X153CrMoV12 sample was then investigated.

The cryogenic treatment applied to the Cry-1 sample is presented schematically in Fig. 1.

The dry linear wear test was performed using a CSM brand Anton Paar Instrument Tribometer model test device according to ASTM G133-05 standard. Experiments were carried out at 25 °C, 25.00% humidity, under atmospheric pressure and a 2.00 N load. The load is determined according to the literature. Wear test parameters included: trajectory (full amplitude of sinus): 20.00 mm; maximum linear speed: 50.00 cm/s; frequency: 7.96 Hz; normal load: 2.00 N; stop conditions: 100.00 m; effective stop (meters and acquisition rate): 100.0 Hz; static friction partner: alumina-coated 6-mm ball. In the friction coefficient tests, the coefficients obtained after reaching the steady state were used. A minimum of five readings was taken for the friction coefficient and wear rate of the sample. The wear rate was calculated according to $W_R = W/L$ equation. In the equation W_R = wear rate (mm³/m), W = wear volume (mm3), L = sliding distance (m) (Ref 20).

Wear surfaces, debris on the surfaces, microstructures and energy-dispersive x-ray (EDS) data were analyzed using the FESEM (Quanta FEG 250) device. Samples were etched (100 mL H_2O, 10 g K_3Fe (CN) 6) before scanning electron microscopy (SEM) imaging.

The electrical conductivity measurements of the samples were made on the Alpha-A High-Performance Frequency Analyzer tester. Electrical conductivity measurement fixed values: DC Volt [V] = 0.0000e+00 and AC Volt [Vrms] = 1.000e+00. Rockwell C hardness measurements were carried out on the Bulut Machine Rockwell hardness tester in 11 s under a load of 10 kgf. For each sample, the average of ten different Vickers and Rockwell C hardness measurements was taken. Vickers hardness measurements were carried out on the Metkon Duroline-M microhardness tester under a load of 1000 g for 10 s. Values were taken from ten different regions and averaged for each sample. The carbide sizes and densities in the microstructure were determined using ImageJ analysis software (Fig. 2). The carbide distribution and average carbide size were calculated by scanning the carbides in microstructure with the help of the image analysis program and using the calculation module of the program. Evaluations of the microstructure of the samples and images of worn surfaces, and EDS analyses were conducted using the Quanta FEG 250 SEM. Wear track widths were measured in the wear images and used to calculate wear rates.

3. Results and Discussion

In this section, the results of the experimental results that occur in the mechanical and tribological properties of X153CrMoV12 steel as a result of the cryogenic process are evaluated. The results obtained as a result of the experiments are given in Table 2.

3.1 Microstructure

Optical microscope images (Fig. 3) of the samples subjected to the different heat treatments were examined and it was seen that the carbide size was smaller and more homogeneous in the cryogenic treatment-1 (Cry-1) and cryogenic treatment-2 (Cry-2) samples. In the conventional heat treatment (CHT) sample, the carbide size was accumulated in a region and had a large

Table 1 Heat treatment conditions for X153CrMoV12 cold work tool steel

	Conventional heat treatment (CHT)	Deep cryogenic treatment 1 (Cry-1)	Deep cryogenic treatment 2 (Cry-2)
1	1050 °C/60 min/5 bar	1050 °C/60 min/5 bar	1050 °C/60 min/5 bar
2	1st tempering [150 °C/120 min]	Cryo (−140 °C/120 min)	1st tempering [150 °C/120 min]
3	2nd tempering [500 °C/120 min]	1st tempering [150 °C/120 min]	Cryo (−140 °C/120 min)
4	3rd tempering [520 °C/120 min]	2nd tempering [500 °C/120 min]	2nd tempering [500 °C/120 min]
5	…	3rd tempering [520 °C/120 min]	3rd tempering [520 °C/120 min]

Samples were gradually brought to room temperature after each procedure.
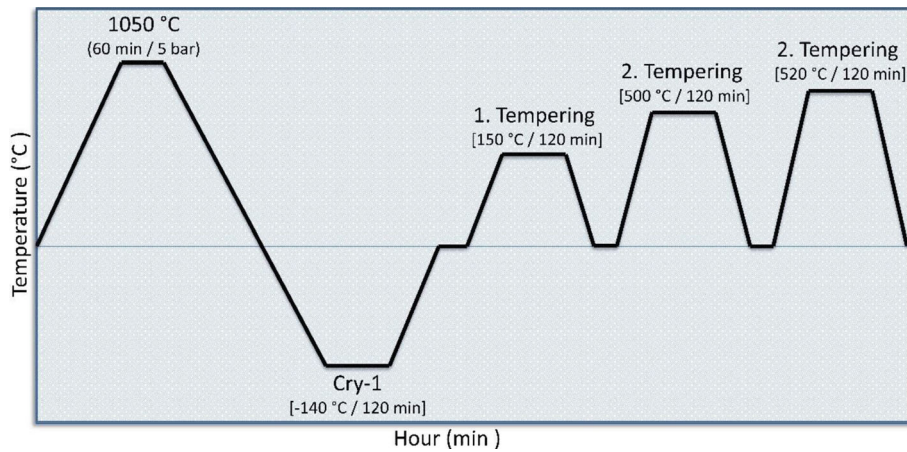

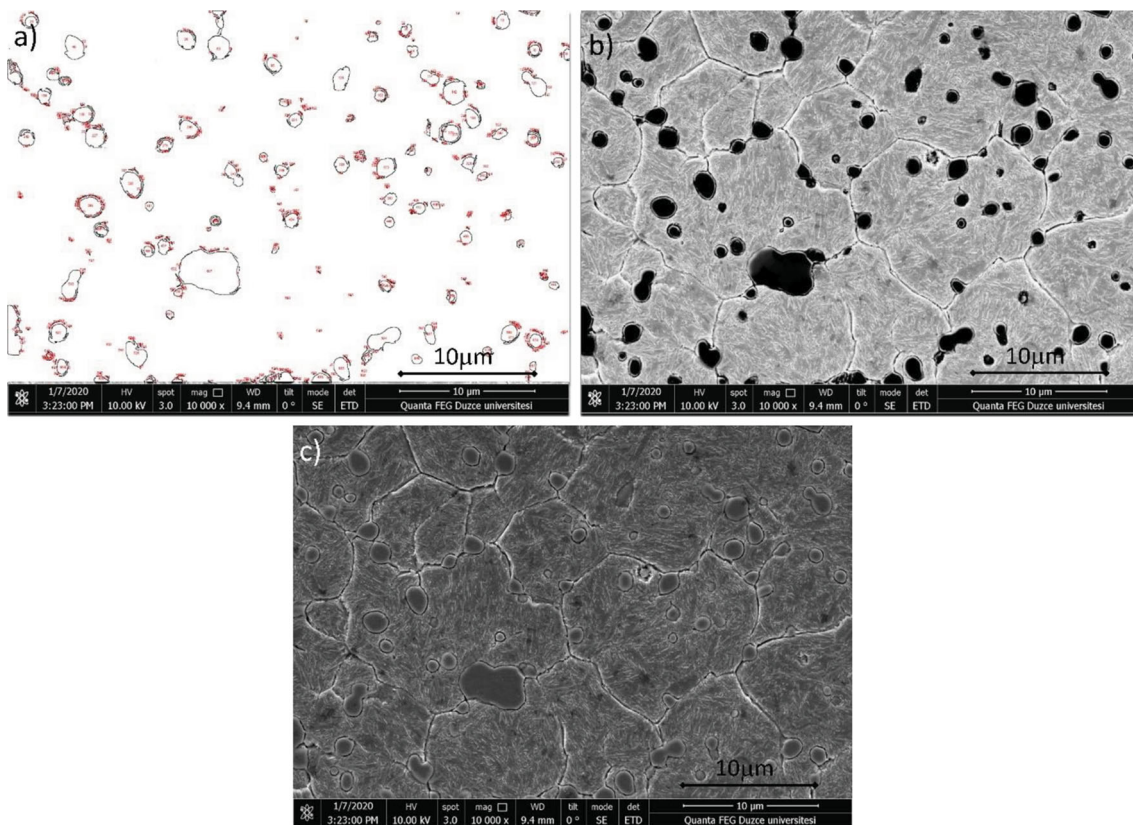**Fig. 1** Schematic presentation of deep cryogenic treatment cycle for Cry-1 sample

Fig. 2 Carbide size calculation with image analysis

Table 2 Summary of results related to hardness values, electrical conductivity, carbide size and wear properties of cryogenically treated X153CrMoV12 steel specimens

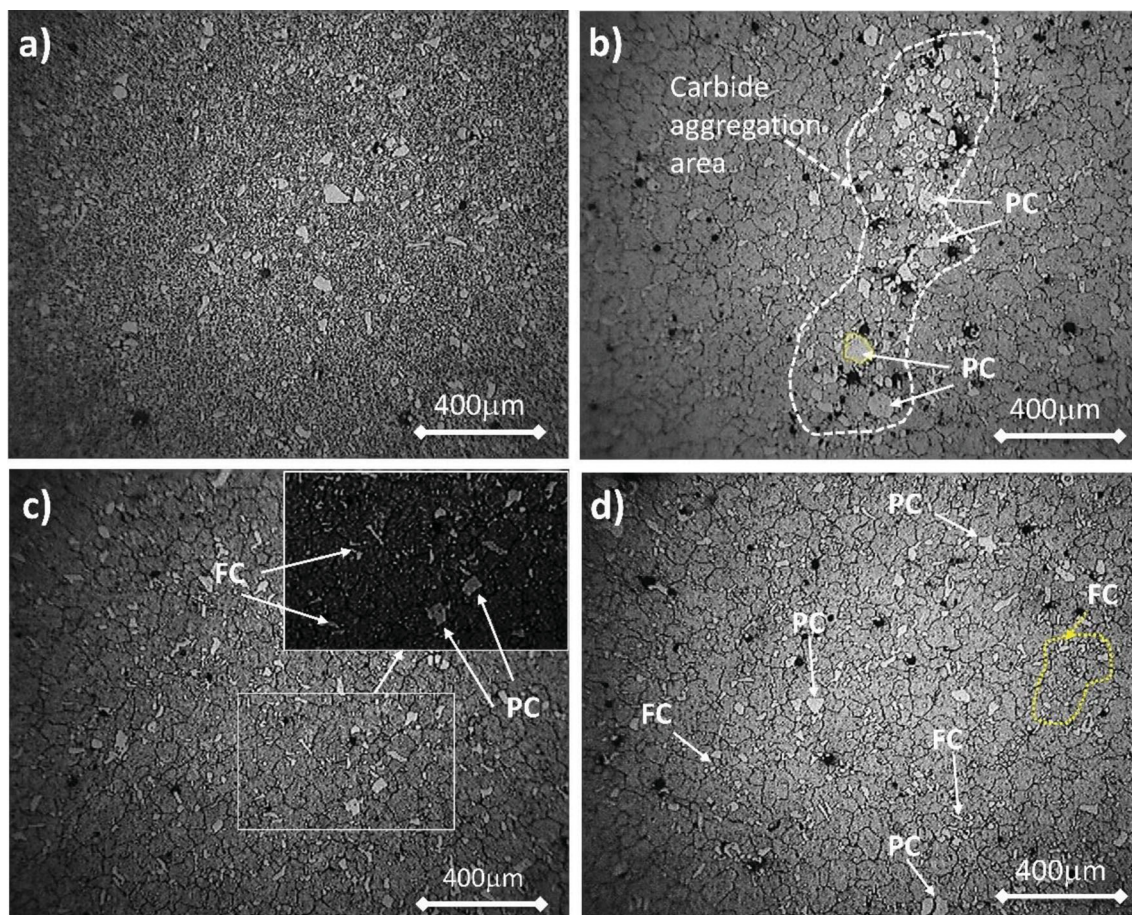| Sample	Mean hardness, HRC	Vickers hardness, HV	Friction coefficient, μ	Wear rate (WR), Nm/mm³	Electrical conductivity, S/cm	Average carbide size, μm
UT	12.96±0.03	209.00 ±0.08	0.096±0.82	5.2430±0.75	2.64E−02	6.939
CHT	58.53±0.02	625.90 ±0.07	0.161±1.18	2.4790±0.78	8.02E+01	6.322
Cry-1	58.83±0.03	678.00 ±0.08	0.168±0.98	1.7440±1.01	2.16E+02	2.045
Cry-2	59.70±0.04	688.00 ±0.10	0.275±1.02	1.6450±0.83	4.65E+02	1.087

Fig. 3 Optical microscope images of samples. (a) UnTreated (UT), (b) CHT, (c) Cry-1 and (d) Cry-2 (PC: primary carbide; FC: fine carbide/secondary carbides)

carbide size structure (Ref 13). Primary carbide (PC) formation in the CHT sample was higher than in the Cry-1 and Cry-2 samples (Ref 18). It has been proven in the literature that the cryogenic process transforms the residual austenite into martensite structure. The heterogeneous structure in the CHT sample and the homogeneous structure in the cryogenic samples can be explained by this change in the microstructure. After the austenite is converted to martensite, the sample is kept in the martensite state for a long time at the cryogenic temperature, producing internal stresses that create crystal defects such as dislocations and twins (Ref 26-28). These changes in the structure of the sample can also explain the homogeneous structure in cryogenic samples.

The EDS analysis was performed to determine the distribution of elements (using the SEM images. The EDS analysis of the CHT samples is given in Fig. 4.

The SEM microstructure images obtained after etching are given in Fig. 5. Primary carbide (PC) formation in the CHT sample was higher than in cryogenic treated samples (Ref 18). Plastic deformation of steels occurs when the dislocation progresses along the crystalline structure. The improvement of the mechanical and tribological properties of steels can be explained by the density of dislocations. Plastic deformation caused by the cryogenic process moves dislocations. This action creates a suitable environment for the formation of new fine carbides (Ref 29, 30). Therefore, PC formation is high in CHT samples. Since fine carbide is formed by cryogenic
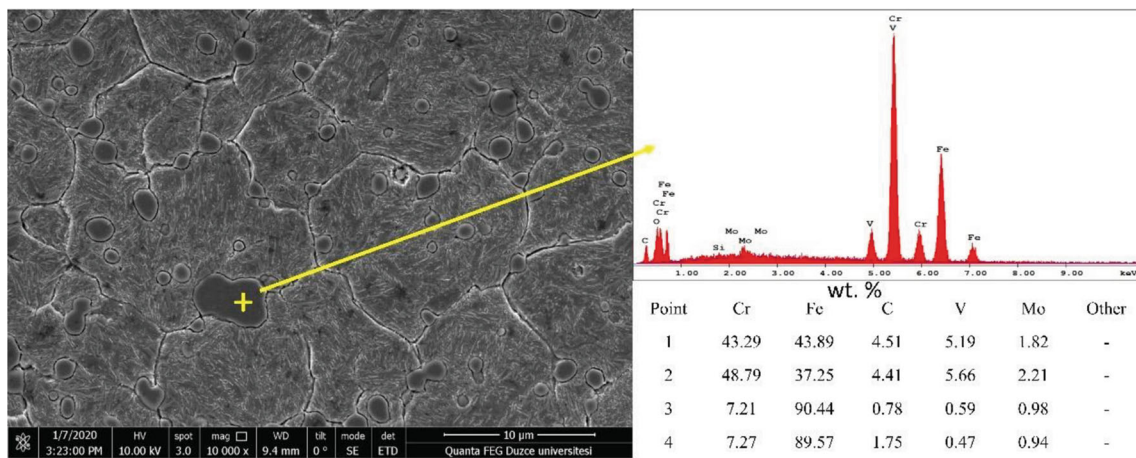
Fig. 4 EDS analysis of CHT samples

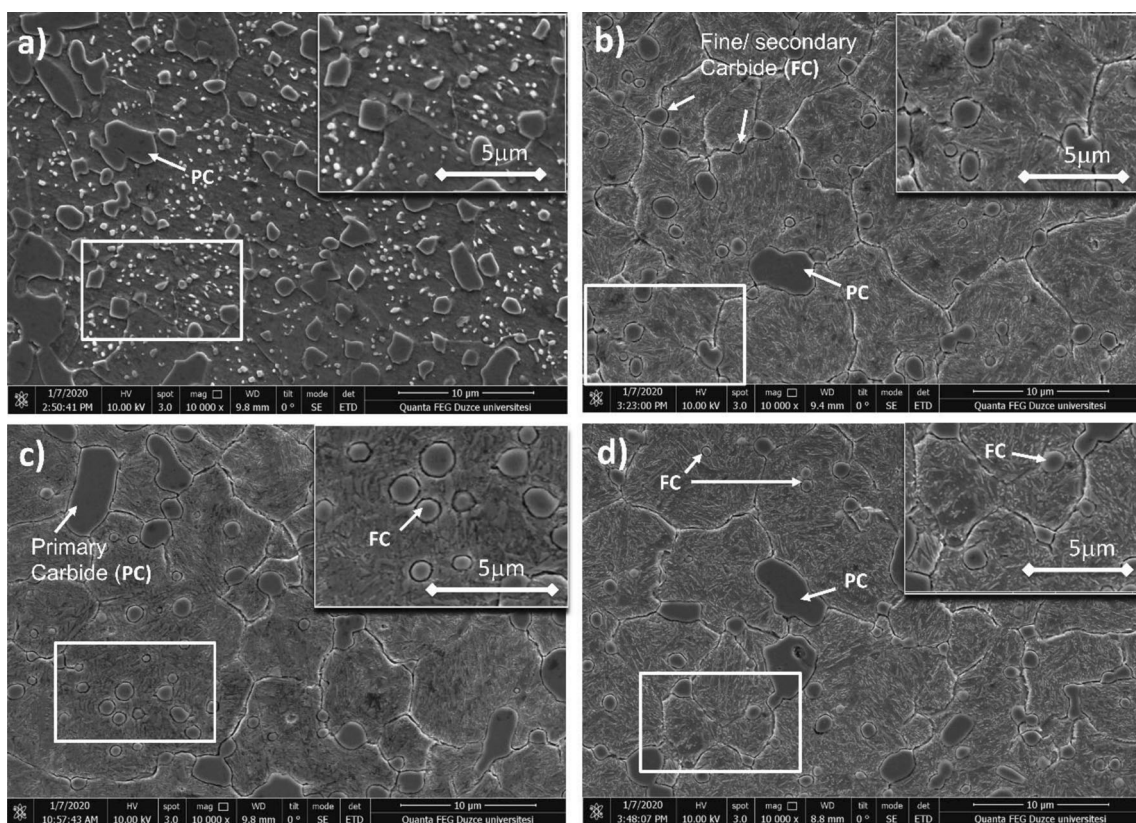| Point	Cr	Fe	C	V	Mo	Other
1	43.29	43.89	4.51	5.19	1.82	-
2	48.79	37.25	4.41	5.66	2.21	-
3	7.21	90.44	0.78	0.59	0.98	-
4	7.27	89.57	1.75	0.47	0.94	-

Fig. 5 SEM images: (a) UT, (b) CHT, (c) Cry-1 and (d) Cry-2 samples. (PC: primary carbide; FC: fine carbide)

treatment, FC is higher in Cry-1 and Cry-2 samples. Amini et al. (Ref 19) reported that the retained austenite in X153CrMoV12 steel was reduced by being transformed into martensite using deep cryogenic treatments and as a result of this, because of high lattice contraction, new fine carbide FC (secondary carbides) was formed. Fine carbides result from microinternal stresses and different expansion coefficients of martensite and neighboring austenite (Ref 28). Cage distortion forces carbon atoms to scatter or separate in nearby crystal defects. These separated regions are known to be new sites for carbide nucleation. These new carbides increase the percentage and homogeneity of carbides in cryogenically treated samples. The researchers also found that due to the deep cryogenic treatment, smaller carbide size was formed and the carbides were distributed more homogeneously (Ref 17). Considering these studies, upon examination of the SEM images, it was seen that the cryogenic treatment produced fine carbide/ secondary carbides (FC) in the Cry-1 and Cry-2 samples and that the primary carbide (PC) was more concentrated in the CHT sample. It was also observed that in the microstructure of the CHT sample, the carbides were scattered and clustered in certain regions (Ref 17, 31).

The EDS mapping analysis (Fig. 6) was performed to observe the microstructure distribution of the elements. An elemental analysis of the whole area was made with EDS mapping. Thus, the distribution of microstructure elements can be seen in more detail. Figure 6(b) shows that in the EDS analysis image of the CHT sample, the Cr is clumped in certain regions. In the Cry-2 sample (Fig. 6(d)), the Cr is distributed more homogeneously. This is consistent with the literature results for the Cry-2 sample where cryogenic purification homogenies the microstructure (Ref 17). However, the same result was not realized for the Cry-1 sample. This shows the importance of the cryogenic process application phase.

According to the results obtained from the microstructures using image analysis software (Table 2), the largest carbide size (6.939 μm) belonged to the untreated (UT) samples. The Cry-2 samples had the lowest carbide size (1.087 μm). This is proof that new, fine carbide had been created. The carbide size in the CHT samples was measured as 6.322 μm.

3.2 Hardness

Because of the importance of hardness and wear resistance, many researchers have studied the effect of DCT on hardness (Ref 32). The Rockwell C and Vickers hardness of the samples are given in Fig. 7. Upon examination, the Rockwell C hardness value of the Cry-2 sample (59.70 HRC) was somewhat higher (Ref 17). The Rockwell C hardness values of the Cry-1 and CHT samples were similar. The Rockwell C hardness value of the Cry-2 sample had increased by 1.5% and 1.9%, respectively, compared to the CHT and Cry-1 samples. The cryogenic treatment did not make much difference in Rockwell C hardness compared to the conventional heat treatment. Das et al. (Ref 2) found in their study (AISI D2) that the cryogenic process increased the hardness by 5%. They reported that this increase was not remarkable. They said that this slight change in hardness could be attributed to the insufficient cryogenic process temperature and cryogenic processing time. They reported that the cryogenic process application parameters did not provide the fine carbide density to increase the hardness. However, a more distinct difference was observed in Vickers hardness values. Although the Vickers hardness value of the Cry-2 sample was 678.0 HV, the Vickers

hardness value of the CHT sample was measured as 625 HV, which shows that there were differences in Vickers hardness. The Vickers hardness value of Cry-2 and Cry-1 sample was 9.9% and 8.3% higher than that of the CHT sample, respectively. The highest Rockwell C hardness value is 59.70 HRC in Cry-2 sample. In the UT sample, this value was measured as 12.96 HRC. This can be explained by the fact that fine carbides were formed with the cryogenic treatment and the microstructure became more homogeneous. FC formed by the cryogenic process contributed to this increase in microhardness. In Fig. 5, SEM images of the samples show the distribution of PC and FC in the microstructures. Amini et al. (Ref 33) found that the microstructure was more homogeneous with deep cryogenic treatment and the new fine carbides formed increased the hardness value. Bensely et al. (Ref 34) by applying deep cryogenic treatment to EN353 steel, they compared the results with conventional heat treatment. They found that the residual austenite transformed into martensite by deep cryogenic processing. As a result, they provided an increase in hardness and wear resistance. Yang et al. (Ref 35) applied deep
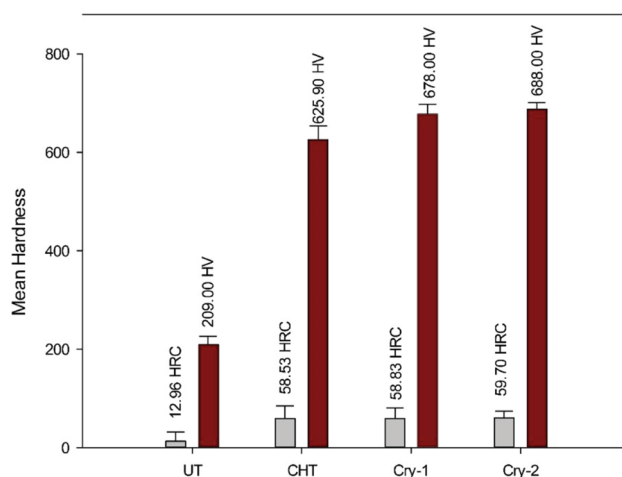

Fig. 7 Summary of results related to Vickers (HV) and Rockwell C hardness (HRC) values
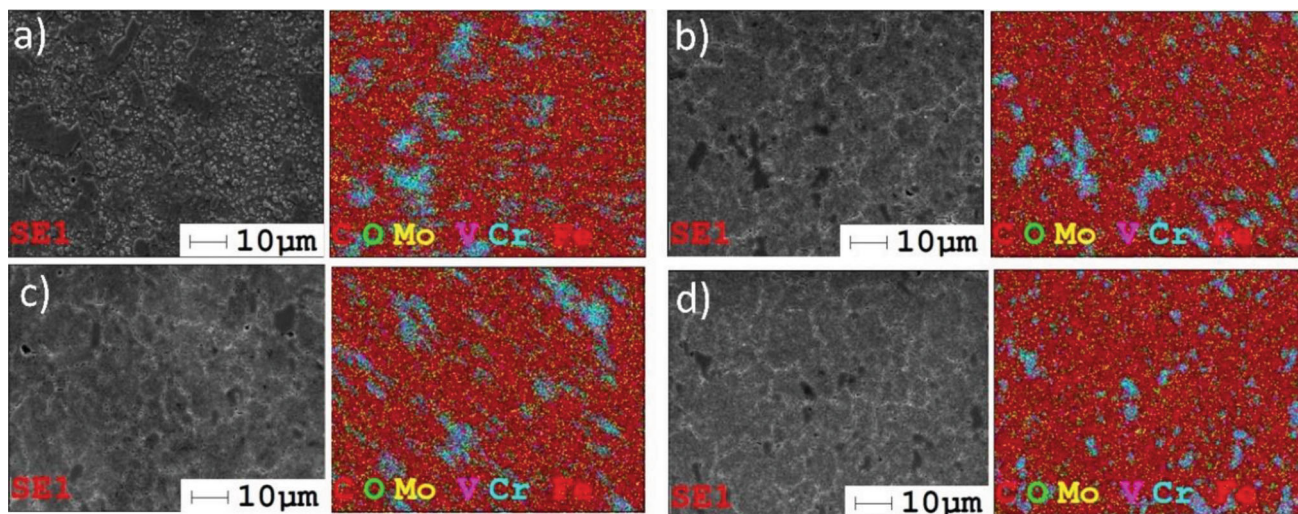

Fig. 6 Elemental (EDS) mapping of images: (a) UT, (b) CHT, (c) Cry-1 and (d) Cry-2

cryogenic treatment to 13Cr2Mn2 V high chromium white iron. They explained the increase in hardness by the transformation of residual austenite to martensite due to the increase in secondary carbides formed in the matrix.

3.3 Wear Behavior

The friction coefficient graph determined by the linear wear test of the Cry-1 sample is given in Fig. 8. The linear abrasion test was conducted on X153CrMoV12 samples and the effect of cryogenic treatment applied in different sequences on wear resistance was investigated. Molinari et al. (Ref 36) applied deep cryogenic treatment to AISI H13 steel. They increased the toughness and wear resistance of the steel by this processing. These properties play an important role in the performance of the steel. The friction coefficient results are given in Table 2. The friction coefficient of the UT, Cry-1, Cry-2 and CHT sample was measured as 0.096 μ, 0.161 μ, 0.168 μ and 0.275 μ, respectively. The mean friction coefficients of the CHT sample and the Cry-1 sample were very close. The friction coefficient of the Cry-2 and Cry-1 sample was 70.8% and 4.3% higher than that of the CHT sample, respectively. This shows that the cryogenic treatment (Cry-2) had an effect on the mean friction coefficient. The cryogenic treatment in the Cry-1 sample was performed before the first tempering and followed by three tempering processes. In the Cry-2 sample, cryogenic treatment was applied after the first tempering process, and then, two temperings were performed. This different application had a positive effect on the friction coefficient of the Cry-2 sample. The Cry-2 sample had the highest hardness among all the samples. It can be said that the homogeneous carbide distribution of fine carbides in the microstructure of the Cry-2 sample had a positive effect on mean friction coefficient.

The graphic showing the wear rates of the samples is given in Fig. 9. The sample with the highest wear rate was UT. The lowest wear rate was achieved by the Cry-2 samples. The wear rate results (Table 2) of the UT, CHT, Cry-1 and Cry-2 samples were measured as 5.2430 Nm/mm^3, 2.4790 Nm/mm^3, 1.7440 Nm/mm^3 and 1.6450 Nm/mm^3, respectively. The cryogenic treatment had a positive effect on the rate of wear. The difference in the wear rate of the Cry-2 sample was determined as 218.7%, 50.7% and 6.0%, respectively, compared to the UT, CHT and Cry-1 samples. Das et al. (Ref 2) found that cryogenic treatment had a positive effect on the wear rate of the X153CrMoV12 sample. They attributed this positive result to

the high wear resistance achieved by the conversion of the structure from austenite to martensite due to the cryogenic treatment. Samuel et al. (Ref 37) applied cryogenic treatment to low carbon steel and found that wear rates decreased with cryogenic treatment. They determined that this effect resulted from the conversion of the structure to martensite via cryogenic treatment. The difference in the wear rate of Cry-2 and Cry-1 sample was 33.6% and 29.6% higher than that of the CHT sample, respectively.

3.4 Worn Surface and Wear Debris

SEM images of the traces formed in the wear tests were examined (Fig. 10). This situation can be explained by the wear rate of the UT sample. Since the abrasion rate is high, the track width is larger. The track widths increased in proportion to the wear rates. Tracks are quite evident in the UT sample in Fig. 10(a). This can be explained by the hardness value and low coefficient of friction of the untreated sample. As the friction coefficients of the samples increased, the wear track widths decreased. The wear track widths of the UT, CHT, Cry-1 and Cry-2 samples were measured as 501.8 μ, 417.0 μ, 381.8 μ and 376.4 μ, respectively. The lowest track width was measured in the Cry-2 sample. The track width of the Cry-2 sample was narrower by 33.3, 10.7 and 1.4%, respectively, compared to the UT, CHT and Cry-1 samples. Because of the ratio between track widths and wear rate, minimal wear occurred in the Cry-2 sample. The track width of Cry-2 and Cry-1 sample was 9.7% and 8.4% higher than that of the CHT sample, respectively. Due to the low wear rate of the Cry-2 specimen, the wear tracks width is also narrow. After the UT sample, the most debris occurred in the CHT sample. Although the hardness values of the samples were close, the wear rates were different, which reveals that the cryogenic treatment contributed positively to the wear rates of the samples. In the UT and CHT samples, the adhesive wear mechanism seemed to be effective. Adhesion wear was higher due to the low hardness in the UT sample. In their study, Das et al. (Ref 18) found adhesion and adhesive wear. The traces formed by the rupture of the adhering parts were wide and deep. Adhesion (Fig. 10(b)) decreased with the increasing hardness in the CHT sample. Accordingly, the depth of the tracks had also decreased. Cryogenic treatment contributed positively to fine carbide formation in the microstructure and homogeneous microstructure wear marks (Ref 19).
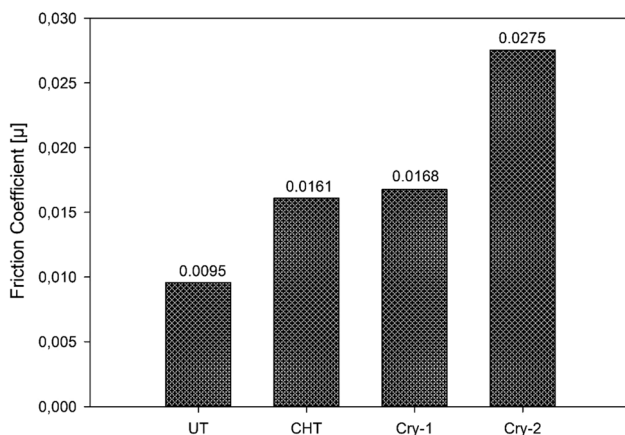

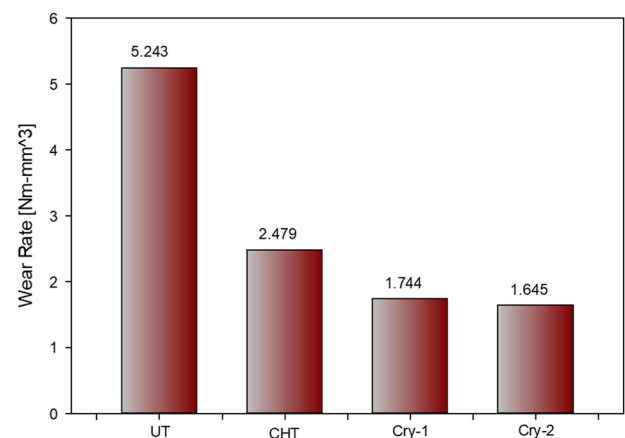**Fig. 8** Friction coefficient results of all samples
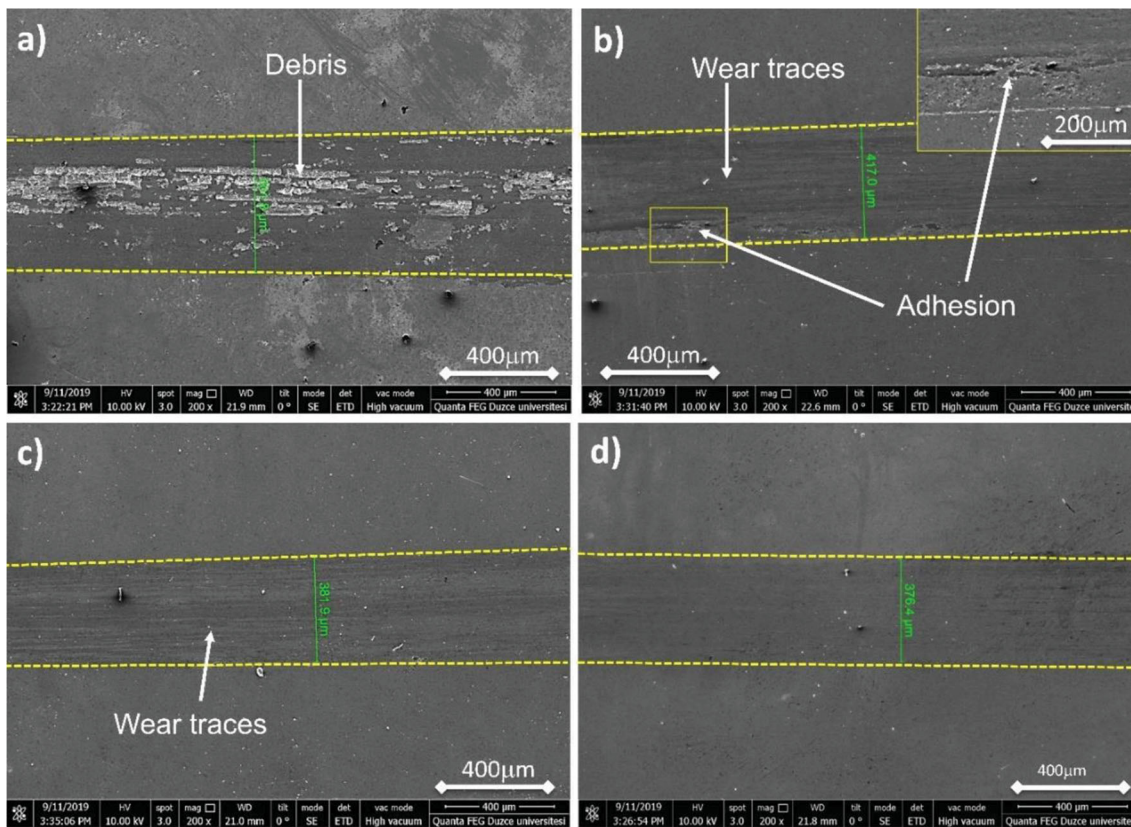

Fig. 9 Wear rate graph of samples

Fig. 10 Worn surface images of samples, (a) UT, (b) CHT, (c) Cry-1 and (d) Cry-2
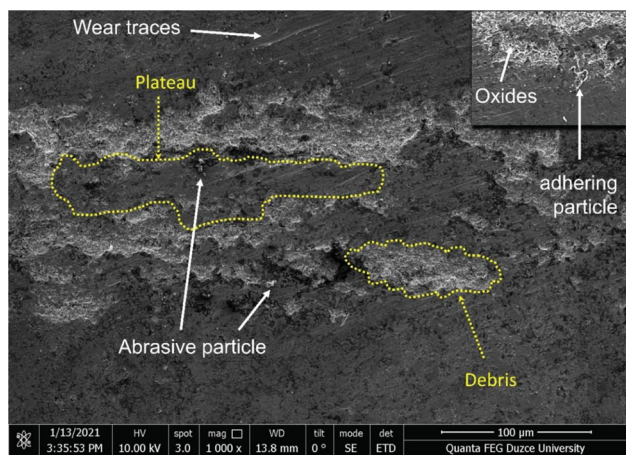

Fig. 11 Worn surface images of UT samples

The depth of the marks formed in the Cry-1 and Cry-2 samples is less.

The worn surface SEM image of the UT sample is shown in Fig. 11. Since the most prominent wear traces are in the UT sample, this image was examined separately to understand the mechanism of wear. The mechanism of wear is not clear, as the wear traces on the CHT, Cry-1 and Cry-2 sample are unclear. According to the wear traces, what is the most obvious wear mechanism abrasive wear. Abrasive wear occurs when the sample is scratched by the grinding effect of small abrasive particles on the sample. This mechanism was particularly

effective in UT samples. Traces caused by abrasive wear mechanism were clearly observed on these samples. In addition, adhesive wear mechanism is also seen in some regions. In the adhesive wear mechanism, the material heated during friction adheres to the sample. As the adhering parts break off, they cause debris in the sample. During the friction test, it is seen that oxide is formed in the debris as a result of the contact of these areas with air. It can be said that these oxides also accelerate the wear (Ref 38, 39). There are very few abrasion traces in the Cry-1 and Cry-1 samples. In other words, the samples did not wear much. This can be explained by the increased hardness of the Cry-1 and Cry-2 samples. It is also known that the cryogenic treatment increases the wear resistance (Ref 40, 41). Since the hardness value of the Cry-2 sample is the highest, the wear is the least in these samples. In this case, it can be concluded that the cryogenic treatment reduces wear. The fine carbides formed by the cryogenic treatment increased the hardness of the samples and reduced their wear. It can be said that the cryogenic treatment applied after the first tempering process in Cry-2 samples has a more positive effect on wear.

3.5 Electrical Conductivity

The effect of cryogenic treatment applications on the electrical conductivity of the samples is shown in Fig. 12. Kalsi et al. (Ref 32) explained that cemented carbide increased their thermal conductivity due to the increase in carbide grain size thanks to the cryogenic process. The increase in thermal conductivity due to cryogenic processing has increased the heat dissipation capacity of cemented carbide. They attributed these to the fact that free electrons are primarily responsible for the
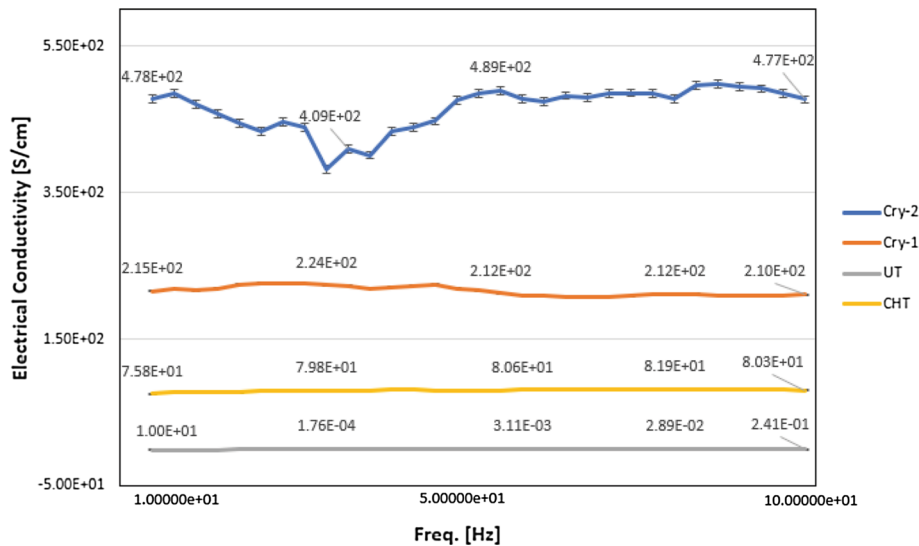
Fig. 12 The electrical conductivity results

electrical and thermal conductivity of metals and alloys. Therefore, the Wiedemann–Franz-Lorenz law relates thermal conductivity to electrical resistivity. The high thermal conductivity of mold steels causes the heat to distribute homogeneously in the mold, especially in injection molds. Therefore, the thermal conductivity of the samples was evaluated by the relationship between electrical conductivity and thermal conductivity results. There was a change in electrical conductivity with the application of different heat treatments. Changes in the microstructure had a positive effect on electrical conductivity. The highest electrical conductivity was achieved in the Cry-2 sample (6.66×10^{02} S/cm), while the lowest was obtained in the UT sample (2.64×10^{-02} S/cm). The electrical conductivity of the cryogenically treated samples was higher than that of the CHT samples. This demonstrated that compared with conventional heat treatment, the cryogenic treatment contributed positively to the electrical conductivity. This may be attributed to the homogeneous microstructure and fine carbide formation (Ref 12).

4. Conclusions

This study investigated the effect of deep cryogenic treatment (-140 °C) applied to X153CrMoV12 cold work tool steel in different sequences. As a result of the research, the following results were obtained:

- A more homogeneous microstructure was obtained with the new fine carbide formed by the cryogenic treatment. Because of these developments, the friction coefficient of the Cry-2 samples was increased, and wear rates were reduced.
- The application of deep cryogenic treatment after the first tempering process (Cry-2) had a positive effect on the hardness. The microhardness value of Cry-2 and Cry-1 sample was 9.9% and 8.3% higher than that of the CHT sample, respectively. There was not much change in Rockwell C hardness values.
- The friction coefficient of the Cry-2 and Cry-1 sample

was 70.8% and 4.3% higher than that of the CHT sample, respectively. Fine carbide (FC) was formed in the Cry-2 samples, and the carbide distribution was more homogeneous.
- According to microstructure studies, primary carbide (PC) was more concentrated in the CHT sample. It can be said that the friction coefficient of the Cry-2 sample has improved thanks to FC formation.
- Minimal wear rate was observed in the Cry-2 sample. The difference in the wear rate of Cry-2 and Cry-1 sample was 33.6% and 29.6% higher than that of the CHT sample, respectively.
- According to the worn surface analysis, the wear track width of Cry-2 and Cry-1 sample was 9.7% and 8.4% higher than that of the CHT sample, respectively. Also according to SEM images, there was less wear on the Cry-1 and Cry-2 samples. Wear traces are more evident in CHT samples. The abrasive mechanism has been effective on the worn surfaces.
- Changes in the microstructure, thanks to the deep cryogenic process, had a positive effect on electrical conductivity. The highest electrical conductivity was achieved in the Cry-2 sample (6.66×10^{02} S/cm), while the lowest electrical conductivity was obtained in the UT sample (2.64×10^{-02} S/cm).

References

1. S. Akincioğlu, H. Gökkaya and İ Uygur, A Review of Cryogenic Treatment on Cutting Tools, *Int. J. Adv. Manuf. Technol.*, 2015, **78**(9–12), p 1609–1627

2. D. Das, A. Dutta, V. Toppo and K. Ray, Effect of Deep Cryogenic Treatment on the Carbide Precipitation and Tribological Behavior of D2 Steel, *Mater. Manuf. Processes*, 2007, **22**(4), p 474–480

3. N. Dhokey, A. Hake, S. Kadu, I. Bhoskar and G. Dey, Influence of Cryoprocessing on Mechanism of Carbide Development in Cobalt-Bearing High-Speed Steel (M35), *Metall. Mater. Trans. A*, 2014, **45**(3), p 1508–1516

4. Y. Li, N. Tao and K. Lu, Microstructural Evolution and Nanostructure Formation in Copper During Dynamic Plastic Deformation at Cryogenic Temperatures, *Acta Mater.*, 2008, **56**(2), p 230–241

5. N. Nayan, S.N. Murty, A.K. Jha, B. Pant, S. Sharma, K.M. George and G. Sastry, Mechanical Properties of Aluminium–Copper–Lithium Alloy AA2195 at Cryogenic Temperatures, *Mater. Des.*, 2014, **58**, p 445–450

6. F. Kara, M. Karabatak, M. Ayyıldız and E. Nas, Effect of Machinability, Microstructure and Hardness of Deep Cryogenic Treatment in Hard Turning of AISI D2 Steel with Ceramic Cutting, *J. Mater. Res. Technol.*, 2020, **9**(1), p 969–983

7. R. Sola, P. Veronesi, R. Giovanardi, A. Forti and G. Parigi, Effect of Heat Treatment Before Cryogenic Cooling on the Proprieties of AISI M2 Steel, *Metall. Ital.*, 2017, **10**, p 5–16

8. R. Sola, R. Giovanardi, G. Parigi and P. Veronesi, A Novel Methods for Fracture Toughness Evaluation of Tool Steels with Post-tempering Cryogenic Treatment, *Metals*, 2017, **7**(3), p 75

9. N. Dhokey and S. Nirbhavne, Dry Sliding Wear of Cryotreated Multiple Tempered D-3 Tool Steel, *J. Mater. Process. Technol.*, 2009, **209**(3), p 1484–1490

10. A.J. Vimal, A. Bensely, D.M. Lal and K. Srinivasan, Deep Cryogenic Treatment Improves Wear Resistance of En 31 Steel, *Mater. Manuf. Processes*, 2008, **23**(4), p 369–376

11. S. Akıncıoğlu, Investigation of the Effect of Shallow Cryogenic Treatment on the Mechanical Properties of 410 Stainless Steel, *Düzce Üniversitesi Bilim ve Teknoloji Dergisi*, 2019, **7**(3), p 985–993

12. S. Akıncıoğlu, H. Gökkaya and İ Uygur, The Effects of Cryogenic-Treated Carbide Tools on Tool Wear and Surface Roughness of Turning of Hastelloy C22 Based on Taguchi Method, *Int. J. Adv. Manuf. Technol.*, 2016, **82**(1–4), p 303–314

13. S. Salunkhe, D. Fabijanic, J. Nayak and P. Hodgson, Effect of Single and Double Austenitization Treatments on the Microstructure and Hardness of AISI D2 Tool Steel, *Mater. Today Proc.*, 2015, **2**(4–5), p 1901–1906

14. G. Akıncıoğlu, F. Mendi, A. Çiçek and S. Akıncıoğlu, Taguchi Optimization of Machining Parameters in Drilling of AISI D2 Steel Using Cryo-Treated Carbide Drills, *Sādhanā*, 2017, **42**(2), p 213–222

15. F. Kara, A. Çiçek and H. Demir, Multiple Regression and ANN Models for Surface Qualification of Cryogenically-Treated AISI 52100 Bearing Steel, *J. Balkan Tribol. Assoc.*, 2013, **19**(4), p 570–584

16. A. Çiçek, F. Kara, T. Kıvak, E. Ekici and I. Uygur, Effects of Deep Cryogenic Treatment on the Wear Resistance and Mechanical Properties of AISI H13 Hot-Work Tool Steel, *J. Mater. Eng. Perform.*, 2015, **24**(11), p 4431–4439

17. K. Amini, S. Nategh and A. Shafyei, Influence of Different Cryotreatments on Tribological Behavior of 80CrMo12 5 Cold Work Tool Steel, *Mater. Des.*, 2010, **31**(10), p 4666–4675

18. D. Das, A. Dutta and K. Ray, Correlation of Microstructure with Wear Behaviour of Deep Cryogenically Treated AISI D2 Steel, *Wear*, 2009, **267**(9–10), p 1371–1380

19. K. Amini, A. Akhbarizadeh and S. Javadpour, Effect of Deep Cryogenic Treatment on the Formation of Nano-Sized Carbides and the Wear Behavior of D2 Tool Steel, *Int. J. Miner. Metall. Mater.*, 2012, **19**(9), p 795–799

20. D. Korade, K. Ramana, K. Jagtap and N. Dhokey, Effect of Deep Cryogenic Treatment on Tribological Behaviour of D2 Tool Steel-an Experimental Investigation, *Mater. Today Proc.*, 2017, **4**(8), p 7665–7673

21. A. Oppenkowski, S. Weber and W. Theisen, Evaluation of Factors Influencing Deep Cryogenic Treatment that Affect the Properties of Tool Steels, *J. Mater. Process. Technol.*, 2010, **210**(14), p 1949–1955

22. I. Gunes, A. Cicek, K. Aslantas and F. Kara, Effect of Deep Cryogenic Treatment on Wear Resistance of AISI 52100 Bearing Steel, *Trans. Indian Inst. Met.*, 2014, **67**(6), p 909–917

23. D. Das, A. Dutta and K. Ray, Optimization of the Duration of Cryogenic Processing to Maximize Wear Resistance of AISI D2 Steel, *Cryogenics*, 2009, **49**(5), p 176–184

24. H. Ghasemi-Nanesa and M. Jahazi, Simultaneous Enhancement of Strength and Ductility in Cryogenically Treated AISI D2 Tool Steel, *Mater. Sci. Eng. A*, 2014, **598**, p 413–419

25. C.H. Surberg, P. Stratton and K. Lingenhöle, The Effect of Some Heat Treatment Parameters on the Dimensional Stability of AISI D2, *Cryogenics*, 2008, **48**(1–2), p 42–47

26. J.Y. Huang, Y.T. Zhu, X.Z. Liao, I.J. Beyerlein, M.A. Bourke and T.E. Mitchell, Microstructure of Cryogenic Treated M2 Tool Steel, *Mater. Sci. Eng. A*, 2003, **339**(1), p 241–244

27. D. Collins, Deep Cryogenic Treatment of Tool Steels: A Review, *Heat Treat. Metals*, 1996, p 2

28. D. Das, A. Dutta and K. Ray, Influence of Varied Cryotreatment on the Wear Behavior of AISI D2 Steel, *Wear*, 2009, **266**(1–2), p 297–309

29. A. Tyshchenko, W. Theisen, A. Oppenkowski, S. Siebert, O. Razumov, A. Skoblik, V. Sirosh, Y.N. Petrov and V. Gavriljuk, Low-Temperature Martensitic Transformation and Deep Cryogenic Treatment of a Tool Steel, *Mater. Sci. Eng. A*, 2010, **527**(26), p 7027–7039

30. S. Li, L. Deng, X. Wu, H. Wang and N. Min, Effect of Deep Cryogenic Treatment on Internal Friction Behaviors of Cold Work Die Steel and Their Experimental Explanation by Coupling Model, *Mater. Sci. Eng. A*, 2010, **527**(29–30), p 7950–7954

31. J. Huang, Y. Zhu, X. Liao, I. Beyerlein, M. Bourke and T. Mitchell, Microstructure of Cryogenic Treated M2 Tool Steel, *Mater. Sci. Eng. A*, 2003, **339**(1–2), p 241–244

32. N.S. Kalsi, R. Sehgal and V.S. Sharma, Cryogenic Treatment of Tool Materials: A Review, *Mater. Manuf. Processes*, 2010, **25**(10), p 1077–1100

33. K. Amini, A. Akhbarizadeh and S. Javadpour, Investigating the Effect of Holding Duration on the Microstructure of 1.2080 Tool Steel During the Deep Cryogenic Heat Treatment, *Vacuum*, 2012, **86**(10), p 1534–1540

34. A. Bensely, A. Prabhakaran, D.M. Lal and G. Nagarajan, Enhancing the Wear Resistance of Case Carburized Steel (En 353) by Cryogenic Treatment, *Cryogenics*, 2005, **45**(12), p 747–754

35. H.-S. Yang, W. Jun, S. Bao-Luo, L. Hao-Huai, G. Sheng-Ji and H. Si-Jiu, Effect of Cryogenic Treatment on the Matrix Structure and Abrasion Resistance of White Cast Iron Subjected to Destabilization Treatment, *Wear*, 2006, **261**(10), p 1150–1154

36. A. Molinari, M. Pellizzari, S. Gialanella, G. Straffelini and K. Stiasny, Effect of Deep Cryogenic Treatment on the Mechanical Properties of Tool Steels, *J. Mater. Process. Technol.*, 2001, **118**(1–3), p 350–355

37. A.P. Samuel and S. Arul, Effect of Cryogenic Treatment on the Mechanical Properties of Low Carbon Steel IS 2062, *Mater. Today Proc.*, 2018, **5**(11), p 25065–25074

38. D. Das, A. Dutta and K. Ray, On the Refinement of Carbide Precipitates by Cryotreatment in AISI D2 Steel, *Phil. Mag.*, 2009, **89**(1), p 55–76

39. B. Kurşuncu, The Effect of Cryogenic Treatment on Dry Sliding Wear Mechanisms in Hard Coatings, *Ind. Lubr. Tribol.*, 2020, **73**(1), p 97–102

40. S.J. Gobbi, V.J. Gobbi, G. Reinke, P.V. Muterlle and D.M. Rosa, Ultra-Low-Temperature Process Effects on Microscale Abrasion of Tool Steel AISI D2, *Mater. Sci. Technol.*, 2019, **35**(11), p 1355–1364

41. S. Kumar, M. Nagraj, A. Bongale and N. Khedkar, Deep Cryogenic Treatment of AISI M2 Tool Steel and Optimisation of Its Wear Characteristics Using Taguchi's Approach, *Arab. J. Sci. Eng.*, 2018, **43**(9), p 4917–4929